Fole 1

JOURNAL OF GEOPHYSICAL RESEARCH, VOL. 91, NO. B10, PAGES 10,443-10,456, SEPTEMBER 10, 1986

GEOELECTRICAL STRUCTURE OF THE NORTHERN PART OF THE SENEGAL BASIN FROM JOINT INTERPRETATION OF MAGNETOTELLURIC AND GEOMAGNETIC DATA

Michel Ritz and Jacques Vassal

Office de la Recherche Scientifique et Technique Outre-Mer, Dakar, Senegal

Abstract. Magnetotelluric (MT) and differential geomagnetic sounding (DGS) surveys were made in the Senegal basin, West Africa, to investigate the conductivity structure of the crust and upper mantle. Magnetic and electric variations were recorded at 11 sites along a east-west profile 220 km in length. The period range of the measurements was 10-10,000 s. For the western stations, the MT response displays low skew with moderate anisotropy. The DGS data indicate the presence of an anomalous geomagnetic variation field in the deep basin and on the eastern margin of our study area. A telluric current concentration in the thick, conductive sediments of the deep basin might cause this anomaly. Both MT and DGS data are then compared with two-dimensional model results to explain the observed features along the profile. Results reveal a strong anomalous crustal structure in the central part of the profile involving a conductive zone (2 ohm m) at depths in the range 4-23 km. Within the deep basin the results of the two-dimensional modeling are not conclusive; acceptable fits between observed and calculated data have been obtained with alternate models. A continuous conductive zone (0.7-2 ohm m) may exist beneath the uppermost layers at a depth of approximatively 1 km, but the observed data can be explained equally well by poorly conducting material intruded into the highly conductive sedimentary cover. This ambiguity is inherent in the two-dimensional models themselves. Both models show that the sediments increase westward to reach a thickness greater than 4000 m when approaching the coast. It is suggested that the flow of current observed in this study is largely controlled by strong lateral variation in the resistivity of the basin and/or by variation of the sedimentary thickness. The models also indicate the existence of two decreased resistivity layers in the eastern part of the profile, one at the base of the crust and the second at 80 km with a resistivity of 20 ohm m. No such layers were detected at these depths below the deep basin. At some depth greater than 150 km there is a general trend toward lower resistivities from 2000 to about 2 ohm m across the entire profile. This may indicate the presence of a small degree of partial melt.

Introduction

In 1980 the Institut Francais de Recherche Scientifique pour le Developpement en Cooperation (ORSTOM) undertook electromagnetic surveys to examine the regional electrical structure of the Senegal basin. As part of this program, magnetotelluric (MT) soundings were carried out to contribute to the knowledge of the structure, thickness and extent of the sedimentary basin. An MT profile made through the central basin and extending along the 14th parallel has shown that the thickness of sediments rapidly increases seaward, and the bulk resistivity of the basin materials was defined in terms of the brine chemistry and porosity with well-conducting sediments [Ritz and Flicoteaux, 1985]. The results have also indicated that the upper crust of the eastern margin of the deep basin displays a surprisingly enhanced electrical conductivity considering its geological and tectonic history [Ritz, 1984].

With a view to learning if this well-conducting structure detected by the MT soundings in the upper crust continues northward and to extend the electromagnetic coverage of the Senegal basin, a 220-km second profile was formed during 1983 from 11 soundings along the 15°30th parallel from Leona (LEO) to Yonofere (YON), perpendicular to the north-south dominant geologic trend of the basin (Figure 1). Both magnetotelluric and differential geomagnetic sounding surveys were conducted in the northern Senegal basin. The site spacing was 20-25 km, and the locations are listed in Table 1. Significant contrasts in resistivity were expected, sufficient to separate the basin sediments from the basement. For the supposed type of conductivity anomaly at a shallow depth and for studying the deep crustal and upper mantle structures beneath, a broad period range of the electromagnetic investigation was envisaged for each sounding. On the west end of the profile the presence of thick conducting sediments at sites will probably screen the electromagnetic response of the upper mantle and inhibit a precise resolution of the resistivity of the upper mantle. For each site of the profile recordings were made simultaneously at two reference stations (BAR and LIN) to provide an estimate of the anomalous geomagnetic variation field [Babour et al., 1976].

This paper describes and analyzes the 11 measurements and presents the results of two-dimensional modeling of data, whereas the geological and tectonic implications linked to the conductivity distribution along the profile will appear in a subsequent publication.

Geophysical Background

The basin is poorly known from its surface geology, and the main knowledge of the basin comes from drilling [De Spengler et al., 1966], electrical soundings [Mathiez and Huot, 1966], aeromagnetic profiles [Bureau de Recherches Petrolieres (BRP), 1956], gravity studies [Crenn and Rechenmann, 1965; Liger and Roussel, 1979; Liger, 1980; Roussel and Liger, 1983] and

Paper number 6B6000.
0148-0227/86/006B-6000$05.00

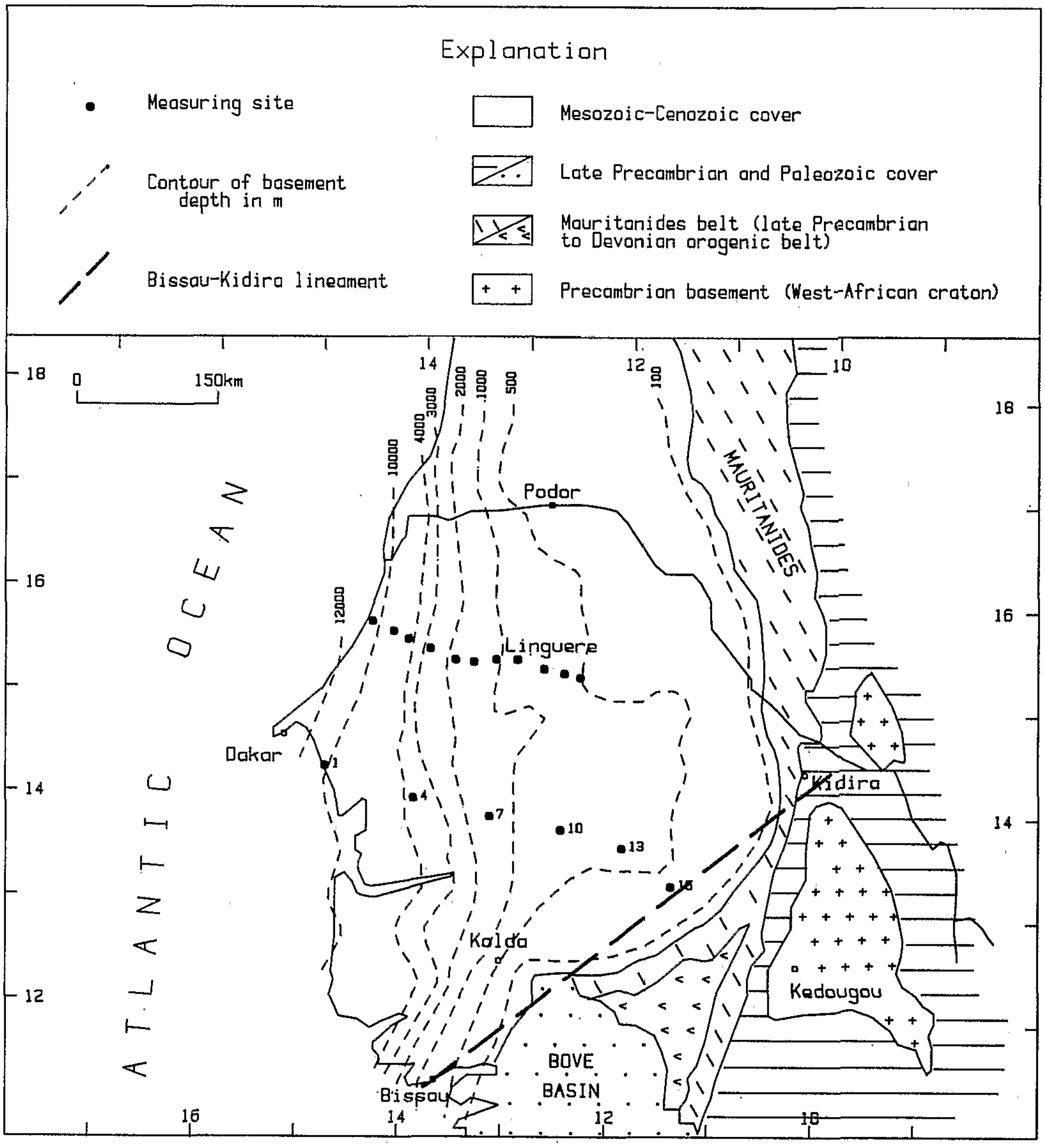

Fig. 1. Index and simplified geological map of the Meso-Cenozoic Senegal basin, showing the location of the measuring sites. Data from sites 1 to 15 were interpreted by Ritz [1984].

seismic refraction profiles [Wyrobek, 1960]. From east to west the Paleozoic-Precambrian basement dips under the Meso-Cenozoic Senegal basin. But the western extension of the partly metamorphic basement under the sediment basin is only known to within a certain depth range because of the limitations in the geophysical methods used: the resistant basement, easily visible to the east, disappeared in the west from a zone between 15° and 15°30'W. Drill holes in this zone have reached Lower Cretaceous at about 3000 m, and at the west end of the profile the basin is likely covered with more than 10,000m of post-Paleozoic sediments. Basement depth contours are shown in Figure 1. Triassic rift sediments have not been reported in the Senegal basin. Magnetic and gravity interpretations have indicated that the basement and Meso-Cenozoic cover are contaminated by numerous mafic intrusions. In the coastal zone of Senegal a positive Bouguer gravity anomaly is interpreted as thinned continental crust, whereas oceanic crust is suggested in the Dakar area. The ellipsoidal positive anomaly at site LEO (60-80 mGal) would be caused by volcanic features and interpreted as a Late Cretaceous intrusive batholith [Pascal and Michel, 1967]. The structure of the sedimentary sequence in the region has a dominantly north-south trend and is characterized by linear faults. The combination of faulting and draping of the overlying sediments is probably due to basement complex block faulting.

Experiments

The MT and differential geomagnetic sounding (DGS) equipment was in operation for approximately 4 months during the beginning of 1983. The magnetometers used are Mosnier variometers [Mosnier and Yvetot, 1972] measuring the horizontal components of the transient field. The electric field was measured in the magnetic

TABLE 1. Location of the Stations

Station	Code	Latitude N	Longitude W
Yonofere	YON	15.26	14.47
Diagueli	DIA	15.27	14.65
Barkedji	BAR	15.28	14.85
Linguere	LIN	15.37	15.10
Ngarafe	NGA	15.38	15.28
Dahra	DAH	15.33	15.48
Boulel	BOU	15.38	15.65
Thiamene	THI	15.49	15.87
Ouarak	OUA	15.52	16.07
Louga	LOU	15.62	16.22
Leona	LEO	15.72	16.45

north-south and east-west directions by using lead electrodes buried in the ground 500 m apart. We had four stations equiped with these sensors, connected with a numeric acquisition system drived with internal clock. Data were recorded in two period bands: 600-10 s for the short-period band at 2-s intervals and DC to 300-s period for the long-period band at 6-s intervals. Data were recorded on cassettes, and according to the sampling interval, the recording duration for both the short-period band and the long-period band can be as long as 15 hours and 45 hours, respectively. Total time of data collection at each site varied from 3 days (short-period) to 2 weeks (long-period), depending on the level of magnetic activity. In general, several data sets were recorded in each period band to ensure good signal to noise ratios. After initial quality control on a micro computer, the data were transferred to a mainframe for subsequent analysis.

Data Analysis and Results

As a first step, all field data (electric and magnetic fields) were plotted for a visual examination to select those that are free from obvious technical and recording noise, step functions and have a broad spectral range with a sufficient magnetically active signal level. Simultaneous records were compared to detect any gaps.

MT Study

Following standard procedures [Sims and Bostick, 1969; Vozoff, 1972; Thayer, 1975], the digitized data were processed to yield estimates of the MT impedance tensor in the frequency domain. The data were then rotated into the principal coordinates to calculate relevant MT parameters such as apparent resistivity and phase. The rotation angles for the principal directions were obtained by minimizing the diagonal elements in the impedance tensor and for two-dimensional situations, one axis is parallel (TE mode) and the other perpendicular (TM mode) to the structural strike. Only in the case of one-dimensional structures do both TM mode and TE mode give identical results. Selection was undertaken by using data with predicted coherence (self-consistency between telluric and magnetic components) greater than 0.9. In general, the data possess a low skewness coefficient [Swift, 1967], particularly for the stations located on the deep basin (usually less than 0.10), indicative of a probable lack of three-dimensional conductivity variation. Both rotated apparent resistivity and phase plots as a function of period in the range from 10 to 10,000 s are shown in Figures 2 and 3 for all stations; ranges indicate 90% confidence intervals. The distinction of both principal directions is crucial, and geological control must be adopted to define the regional strike. In the deep basin the dominant trends are north-south, similar trends are evident in the magnetic and gravity data [Liger, 1980]. The lower diagram of Figure 5 shows the electrical impedance strike directions for stations in the survey area for the period of 1000 s; these directions are nearly invariant over all the period range analyzed. It is apparent that the strike changes in a systematic fashion between each site; however, the electrical strike directions are approximately north-south in the study area. The data from all sites except LEO, located at the west end of the profile near the Atlantic coast, are anisotropic in that the major and minor plots are dissimilar. However, for sites THI and OUA the major and minor components of apparent resistivity appear to converge at periods more than 100 s; it can be expected that the two-dimensional conductivity distribution is restricted to the upper few kilometers of the crust, while the deeper conductivity structure is dependent on depth only beneath these sites. The rotated major and rotated minor responses observed at sites YON DIA, and BAR are very different from those observed at any other location. At long periods the major apparent resistivity is of the order of 200 ohm m, and principal phases increase with period from values close to zero degrees to approximately 45°.

A preliminary examination of the major and minor estimates at each site indicates that we may roughly distinguish three different groups of response along the profile, namely, the eastern group including the shallow basin with YON, DIA, and BAR; the central group with LIN, NGA, and DAH; and the western group covering the deep basin with BOU, THI, OUA, LOU, and LEO. The results from these stations are then discussed group by group.

Eastern group. The similarity of the YON, DIA, and BAR responses (amplitude and phase) is striking (Figure 2). The apparent resistivity data display increasing anisotropy with increasing period. The major estimates are approximately an order of magnitude longer than the minor estimates at the long periods. The major curve at site YON is slightly larger than those at DIA and BAR, but the shapes of the curves are similar. According to the major curve at 300-s period there is evidence for a conductor at depths of 70-80 km as the amplitude reaches its minimum value. Data, particularly at BAR, show a pronounced parallel split between the major and minor curves, this splitting is seen only on the amplitude data, and the phase data are not affected. Berdichevsky and Dimitriev [1976] have shown that this splitting is caused by near-surface inhomogeneities of conductivity.

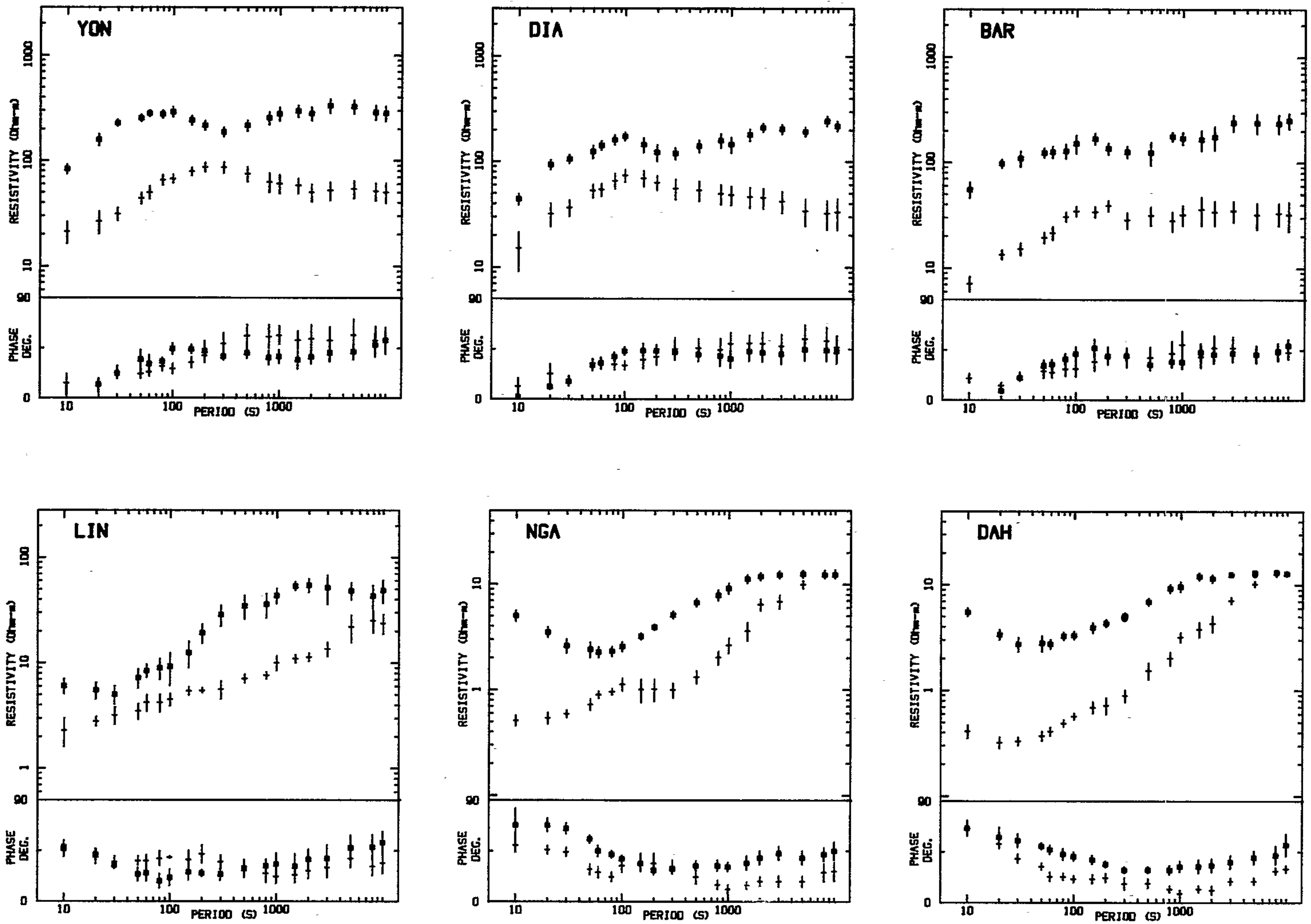

Fig. 2. Tensor resistivity and phase plots for the MT soundings located in the eastern part of the profile.

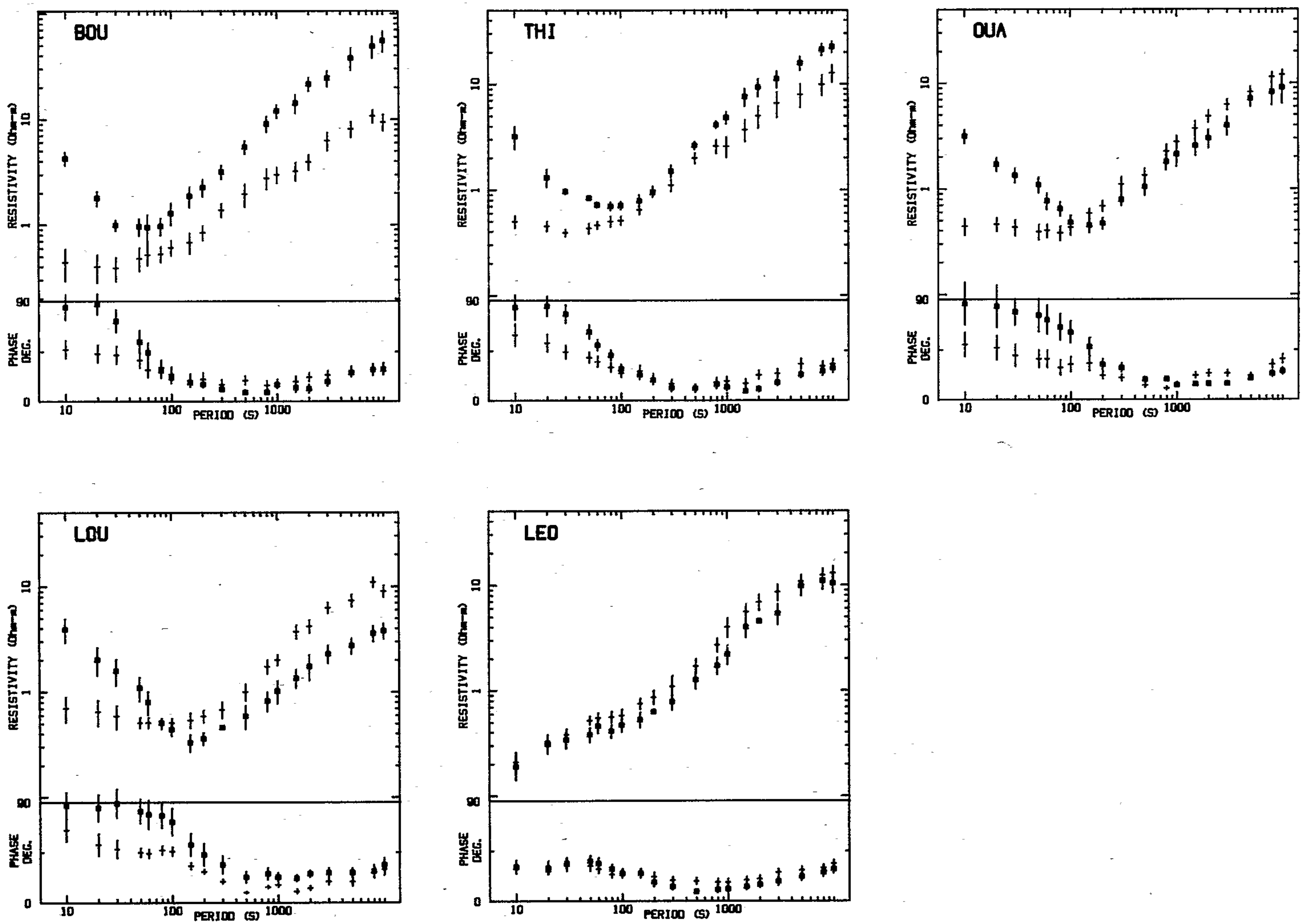

Fig. 3. Continuation of data plots for the westerly stations.

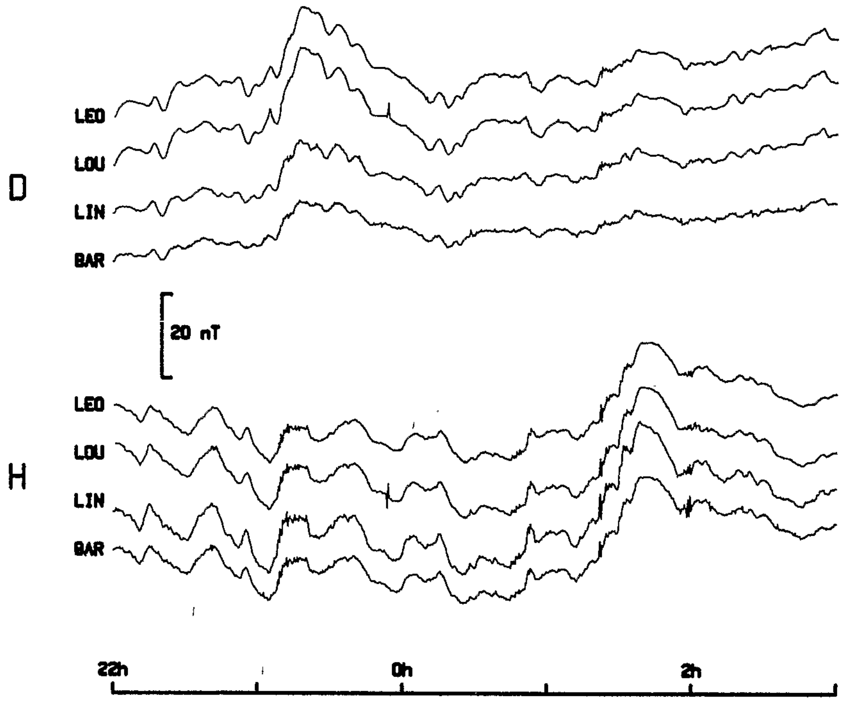

Fig. 4. Simultaneous records of horizontal geomagnetic variations between 2200 hours on May 4, 1983, and 0300 hours on May 5, 1983, from LEO, LOU, LIN, and BAR. Sampling interval was 6 s.

Central group. Of particular significance is the fact that the plots for this group are dramatically different from those recorded at sites in the east. Such difference usually indicates major structural boundaries in the vicinity [Vozoff, 1972], and consequently, these sites must be subject to different structural constraints. Several characteristics of the curves will be important in the interpretation. For example, the major resistivities are more than an order of magnitude smaller than those at sites BAR and DIA in the east. The minor curves at LIN and NGA display a flat part between 100 and 300 s. At DAH this feature is less well defined; a low-amplitude inflection appears in the values of minor apparent resistivity at periods of 80-150 s. However, a more diagnostic response is generated in the phase data which appear flatter in the period range 60-200 s, resembling those at NGA. For NGA and DAH, we observe uniform but small values of apparent resistivity which lie between 0.5 and 10 ohm m. Greater than 50 s the major curves (20 s at LIN) show a distinct rise in the apparent resistivity by 2-10 ohm m (4-60 ohm m at LIN), followed by a slight decrease in apparent resistivity from 2000 s, indicating conductive zones within the upper mantle. It is interesting to note that in the central zone of the basin the sedimentary cover is thin and the pronounced gradient in apparent resistivities between sites BAR and NGA coupled with consistent low apparent resistivities obtained from the central sites probably result in the presence of a crustal conductivity anomaly directly beneath LIN, NGA and DAH.

Western group. The MT results for BOU, THI, OUA, LOU, and LEO which lie on the deep basin are presented in Figure 3. The values of apparent resistivity, in both principal directions, are particularly small in this area and lie between 0.25 and 20 ohm m, except BOU where the major apparent curve reaches values of about 60 ohm m. The degree of anisotropy is relatively small for periods of 100 s and above. At LEO, both major and minor estimates are identical displaying an isotropic conductivity structure. The values of apparent resistivity at LEO are the smallest obtained in this study with values around 0.25 ohm m at 10 s. For the other traverse sites, at 10-s period, the ratio of major to minor resistivities is around 8, indicating lateral variations in the basin structure. From BOU to LOU in the 50-200 s range, the minimum in apparent resistivity curve is in a progressively shifted manner with increasing period, particularly for the major apparent resistivity curves: the minimum value tends to be around 50 s at BOU and around 150 s at LOU. This trend reflects an increasing thickness of basin sediments toward the west. Above 50-150 s, all the major and minor apparent resistivity curves show the same trend with a distinct rise to an apparent resistivity of approximately 1-10 ohm m at the long-period end (with some divergence between the sites). With increasing period, both major and minor phases decrease from values close to 90° to approximately 20° until about 1000 s where they begin to gradually increase to nearly 45° at the longest periods.

Note that at site LEO, which is situated close to the coast line, no coastal effect can be seen in apparent resistivities in the observed period range and there is not a good, high conductivity contrast between the ocean and the land. However,

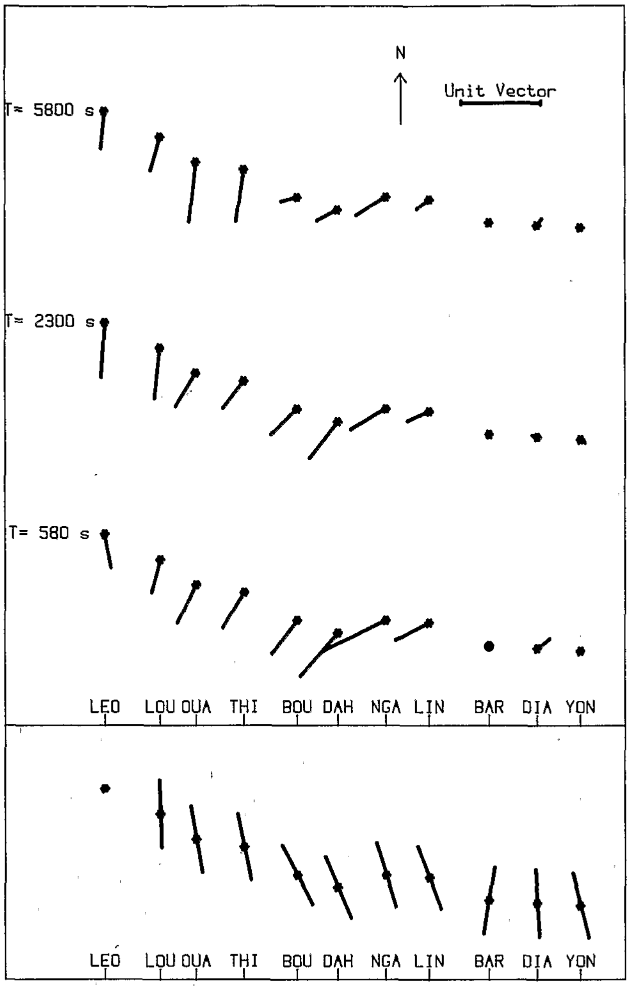

Fig. 5. Upper diagram represents the distribution of telluric current flow responsible for anomalous fields at recording stations. The vectors with arbitrary units are at right angles to the anomalous fields and their length is proportional to the modulus of the anomalous geomagnetic field. Geomagnetic field variations at BAR were chosen as the reference in calculations of the anomalous geomagnetic field across the Senegal basin. On the east end of the profile the anomalous current system almost vanishes. The lower diagram gives impedance strike directions (clockwise from north). The electrical impedance strike direction is indefined at LEO.

pronounced lateral gradients of the resistivity structure may conceal the ocean effect [Beblo et al., 1983].

DGS Study

An example of the observed geomagnetic variations at four recording stations over the Senegal basin is given in Figure 4 where magnetograms (magnetic eastward (D) component and magnetic northward (H) component) are shown for 2200 hours on May 4 to 0300 hours on May 5 at LEO, LOU, LIN, and BAR. Note that the DGS measurements were restricted to the long-period band.

The first step on the analysis of anomalous field is a digital filtering of the raw data. The mathematical filtering used is described by Grillot [1975]. The filtering records are visually inspected, and short sections which show a well-defined signal are picked; on these picked sections, we calculate anomalous vector field

$$\overrightarrow{Hio}(t) = \Delta\overrightarrow{Hio}(t) - \Delta\overrightarrow{Dio}(t)$$

with $\Delta\overrightarrow{Hio}(t)=\overrightarrow{Hi}(t)-\overrightarrow{Ho}(t)$ and $\Delta\overrightarrow{Dio}(t)=\overrightarrow{Di}(t)-\overrightarrow{Do}(t)$, where o is the reference station and i the mobile station.

Since it is not possible for us to have simultaneous recordings at all stations, we had to resort to a normalizing process in order to be able to compare the anomalous field for one group of mobile stations to another at other day. For this purpose, two fixed stations (reference o BAR, reference 1 LIN) were operated during the whole experiment. The component of anomalous field at the station Si will be characterized by the following vector:

$$\overrightarrow{kH}(Si) \left| \begin{array}{l} kh(Si) = \Delta Hio(t)/\sqrt{(\Delta H1o^2(t) + \Delta D1o^2(t))} \\ kd(Si) = \Delta Dio(t)/\sqrt{(\Delta H1o^2(t) + \Delta D1o^2(t))} \end{array} \right.$$

This vector is proportional to the horizontal anomalous field and can be only defined up to a constant multiplicative factor. In practice, we have computed, for each station Si and for each filtered period various values of kH from several samples. For periods longer than 500 s, standard deviations are small, but for periods less than 500s they are approximately 30° in azimuth and 20% in modulus.

In the upper diagram of Figure 5, the distribution of anomalous telluric currents responsible for differential fields is plotted for the periods 580, 2300, and 5800 s for the stations along the profile [Babour et al., 1976; Babour and Mosnier, 1980]. The anomalous geomagnetic variation field across the zone under investigation at sites LIN-LEO is characterized by excessive anomalous current flows in two principal linear features: one which runs approximately westward for the easterly stations and the second runs southward through the deep basin for the westerly stations. The results show that the anomalous character of the horizontal field is maintained over a large distance at periods ranging from 580 to 5800 s. It is clear that for all sites the change in direction is smooth with periods and that there is a significant measure of consistency between adjacent sites. At 580-s period the westerly sites (LEO, LOU, OUA, THI, and BOU) have vectors which are orientated southward and in the south west direction and the easterly (DAH, NGA, and LIN) are more westward. At 5800-s period the vector direction at LEO, LOU, OUA, and THI point south ward, but the easterly stations (BOU, DAH, NGA, and LIN) show vectors which swing westward, particularly for stations BOU and DAH in the center of the profile. At all sites the anomalous geomagnetic field is up to twice as large as the normal field at the reference site BAR, in particular at sites DAH and NGA in the 360-2300 s range. Moreover, there is a definite trend of the decreasing vector amplitude from east to west for periods shorter than 2300s except LIN, whereas periods shorter than 2300s except LIN, whereas the vectors tend to be greater westward for periods longer than 2300 s. In the eastern part of the profile, BOU, DAH, NGA, and LIN appear to be sensitive to period, and there the effect is decrease in strength of the vector with increasing period. Both amplitude and direction are affected. The vectors for periods longer than 2300 s are thus oriented parallel to the major geologic trend at stations LEO, LOU, OUA, and THI inside the deep basin and approximately perpendicular to the major trend at stations BOU, DAH, NGA, and LIN outside the deep basin, as illustred by the direction of the 5800-s vectors, suggesting that the induced telluric currents are controlled by local geological structure. At shorter periods, between the site LIN in the east and the site LEO in the west, the vector swings progressively southward from an initial direction that is about N110°W, indicating the influence of the deep basin. At first glance, it is quite probable that current concentration westward is due to electric currents flowing in the sediments of the Senegal basin parallel to the north-south dominant geologic trend. The eastern stations, with a thin sedimentary cover, act as a resistive area where the current flow is deflected, while it is concentrated by thick well-conducting sediments at the western stations. The observed anomalous field through this zone is probably due to the perturbations in the regional current flow which are created by strong horizontal contrasts in electrical conductivity and variation in depth of the basement within the basin.

For sites DIA and YON the anomalous geomagnetic variation field is negligible, indicating that the field at these stations is not influenced significantly by lateral variations in the regional telluric current system. Note that the direction of anomalous current flow indicates no influences related to the coast effect within the range OUA, LOU, and LEO where LEO is situated close to the coast line [Edwards and Greenhouse, 1975; Parkinson and Jones, 1979].

Conclusions From the Qualitative Interpretation of the Data

The advantages of the joint application of both MT and DGS method are shown by this study. The qualitative interpretation of the results of both techniques suggests that the anisotropy of the MT curves at short periods, and the anomalous horizontal fields can be accounted for by strong lateral gradients of the conductivity distribution and/or the lateral variation of the sedimentary thickness within the basin. A dominant north-south trend exists for both the impedance strike directions and anomalous current flow vectors in the west part of the profile and coincides with the striking direction of the sedimentary cover. Model calculations are clearly needed to determine more accurately the depth and location of this anomalous telluric concentration and associated geoelectrical structure.

Although the MT data interpreted show a high coherence (0.9) between electrical and magnetic components and a dimensional indicator (skew) less than 0.1, suggesting two-dimensional domination, the possibility must be considered that the anomalous field may be due to channel currents which are not related to the local induction process. In fact, two modes of local telluric concentration which cause anomalous fields may occur, namely, the local induction due to a nearby electrically conductive structure (for example, basin sediments) and the regional current channelling by a local conductor of currents generated by induction over a region much larger than the zone under consideration in a three-dimensional geoelectic structure. The importance of determining the nature of the induced currents, currents related to local induction or injected currents, lies in the choice of the type of modeling that may be undertaken to interpret the geoelectric structures responsible for the observed anomalous fields. Nevertheless, the separation of the two effects is a matter of some debate [Beamish and Banks, 1983; Fischer, 1984; Jones, 1983; Dupis and Thera, 1982]. In general, questions on local induction and telluric current concentration can only be answered by solving regional induction in three-dimensional configurations in which the two effects are distinguishable from each other [Vasseur and Weidelt, 1977; Hermance, 1982; Weaver, 1982].

Two-Dimensional Interpretations and Discussion

The responses were inverted by a one-dimensional scheme [Jupp and Vozoff, 1975], and the main features of these resulting models were used as a starting point to construct a number of two-dimensional models [Wannamaker et al., 1985]. All available geological and geophysical evidence was used to place boundaries and provide estimates of sedimentary rock resistivities. It is possible from the calculation of the values of magnetic field for different periods and several sites to obtain the same type of data as was obtained experimentally with DGS. Therefore DGS data were interpreted in terms of geoelectric structure supposing that the anomalous fields are generated by lateral variations in conductivity within the basin; the E along strike component of two-dimensional models is used. The anomalous magnetic fields at each station normalized with respect to the magnetic field at BAR taken as representing the normal field are shown in Figure 7 at the period of 1000 s and were compared to the model results. Based on the qualitative interpretation of the data and the one-dimensional models, we propose a two-dimensional model that is consistent with the MT and DGS observations within the accuracy of the field data (Figure 6). The response of this model at typical sites YON, NGA, and LOU for both the TE mode and TM mode is shown with the observed apparent resistivities and phases in the lower diagram of Figure 7. The agreement is good for the MT estimates. Because the station density is not particularly high and the wide spacing in the measuring area, the model can only be a general one. At DAH, NGA, and LIN a narrow crustal conductor with low resistivity of 2 ohm m buried in an environment of high resistivity (2000 ohm m) is necessary to fit the short-period MT and DGS data, but the computed values for the anomalous fields are slightly larger than observed. These results may be seen in the upper

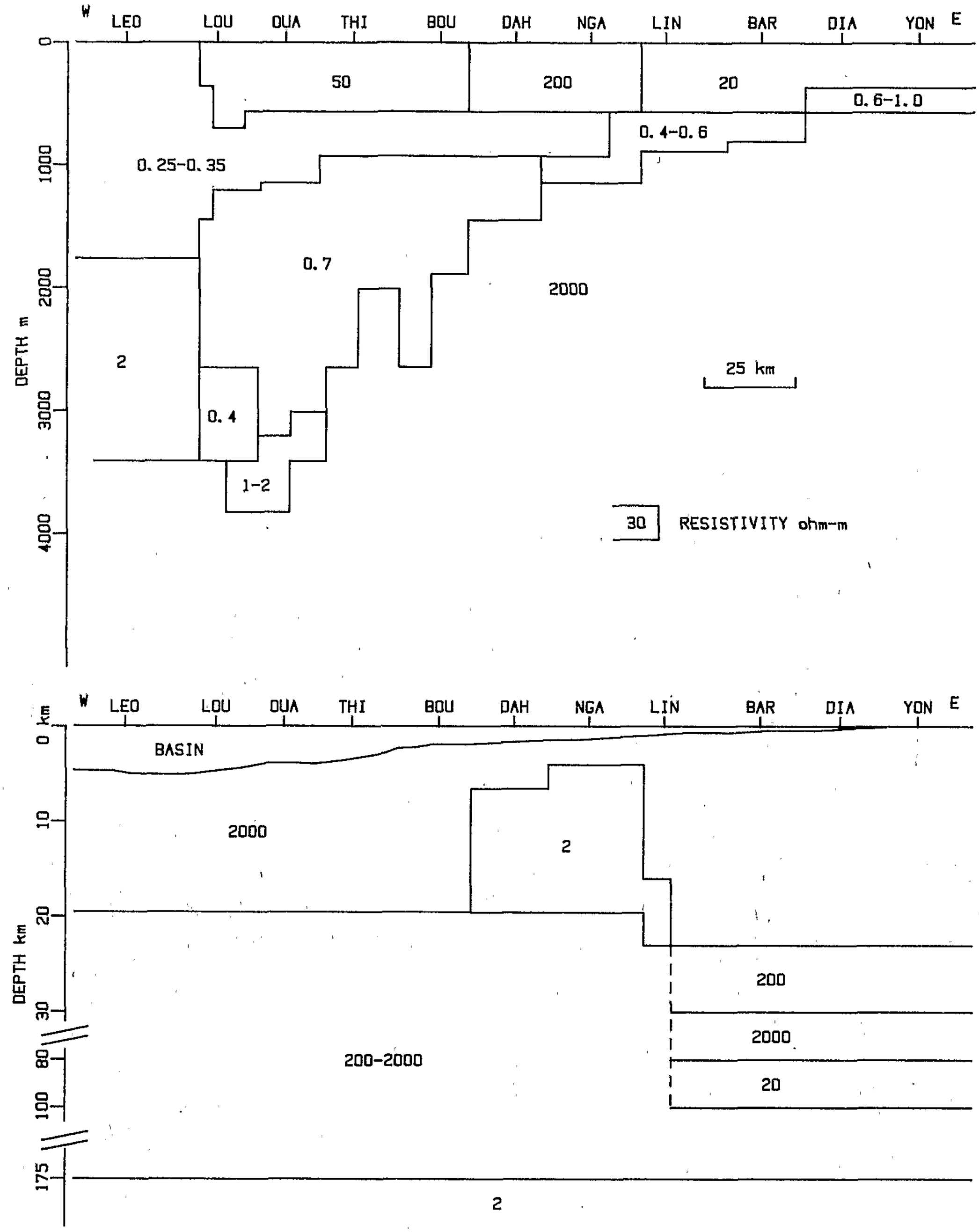

Fig. 6. Model of two-dimensional conductivity distribution at all sites of profile, calculated from both MT and DGS data. The highly inhomogeneous structure of the basin is shown in the upper portion of the figure. The lower graph shows the strong lateral distribution of conductivity in the crust below the central area and the upper mantle electrical structure.

diagram of Figure 7 where the observed anomalous fields are plotted along the profile with the response of the two-dimensional model at a period of 1000 s.

In our survey area, previous to this investigation, two gravity models of the deep structure of the Senegal basin have been proposed by Liger [1980]. The first model was an attempt to explain the gravity data on the basis of intrusions into the sedimentary cover. Note that the position of the high-density rocks correlates with the 200 ohm m blocks at sites LOU and THI shown on the two-dimensional model (upper diagram of Figure 6). In the second gravity model most anomalies were tentatively associated with thick mafic intrusions within the basement. In view of this possibility we have constructed an alternate basin model (Figure 8). The most significant features shown by this model are the smooth lateral changes of resistivity with resistivities increasing with depth below the surface layer (except LOU) and abrupt truncations of the deep conductive material of the basin. The overall fit to the observed data is nearly identical with

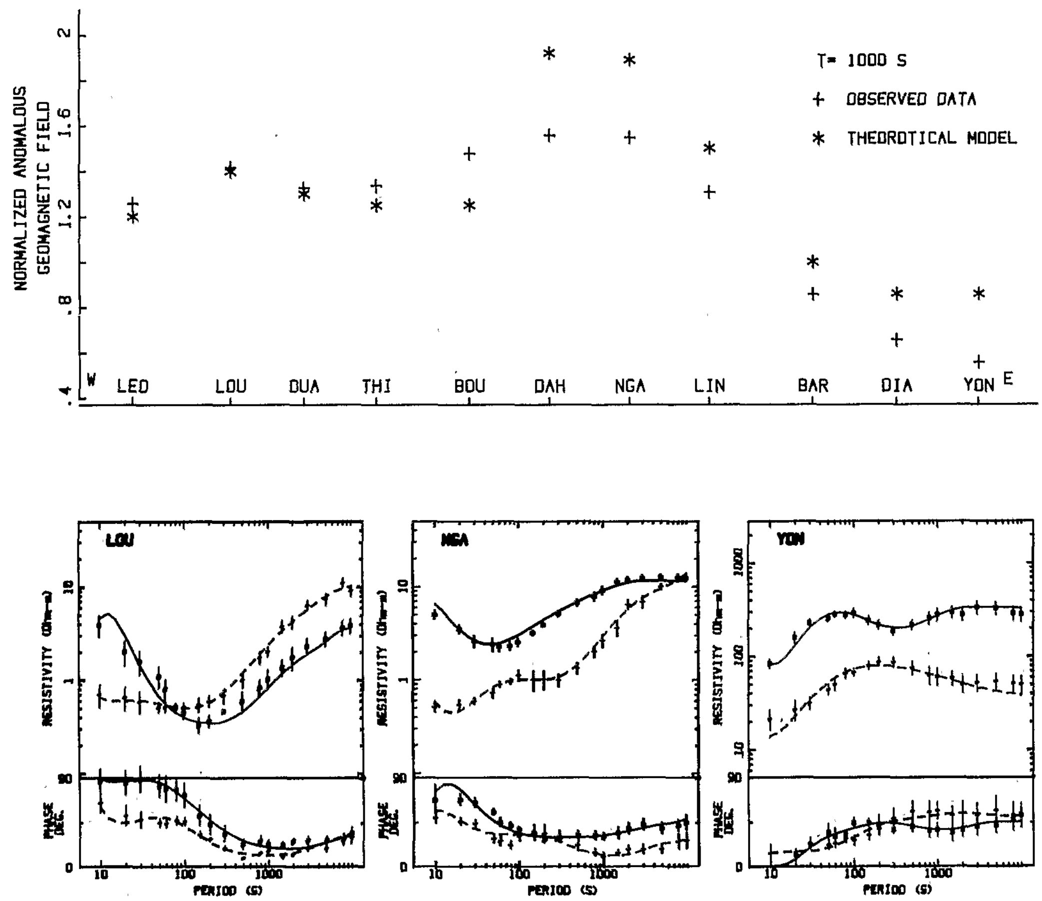

Fig. 7. Results of observation and calculation along a profile perpendicular to electrical strike across the Senegal basin. In the lower diagram the calculated TM (solid curve) and TE (dashed curve) estimates are shown plotted through the measured values for three typical sites YON, NGA, and LOU. Computed (stars) and observed (crosses) anomalous horizontal geomagnetic fields for a 1000-s period are shown in the upper portion of the figure. Anomalous fields are normalized with respect to the normal horizontal geomagnetic field at the reference station BAR.

that for the first model. Although numerical differences occur, they are, for the most part, well within the accuracy of the field results. There is a poor discrimination between the computed resistivity values for the two models. This non uniqueness is inherent in the two-dimensional models themselves and is further complicated by possible effects of regional three-dimensional currents channelling within the conductive sediments of Senegal basin. In the area under study four drilling and well logs are available [Maugis, 1955] and could be useful to elucidate the nature of materials in the sedimentary geoelectric section. The location of the drill holes is shown in Figure 1. The La2, SaFl, and TBl holes were drilled to depths of 1150, 1716, and 4000 m, respectively, and bottomed in sedimentary rocks. They indicate that the Cretaceous sediments are generally poorly consolidated, porous, and electrically conductive. Composition is dominantly sandstones and clay, but some limestones are also encountered. Resistivities lie chiefly in the range 0.3-1.5 ohm m. The Lal hole was drilled to a depth of 710 m and bottomed in resistive rocks of Upper Cretaceous age. This shows the complexity of the sedimentary sequence and could indicate lateral variations of conductivity between holes Lal and La2 in the vicinity of site LEO. The resistive material at a depth of 710 m on the west end of the profile is thought to represent intrusions. The picture of the subsurface provided by well log information is limited to the near vicinity of the borehole. Note that the resistivities deduced from alternate model (Figure 8) show good conformity with the electrical resistivity values from three of the wells (La2, SaFl, and TBl). However, due to the absence of borehole measurements near the MT sites (except LEO), the first model cannot be ruled out as a possible resistivity structure beneath the study area.

The internal geoelectrical structure along the profile can be characterized by the following features:

Sedimentary Basin (Upper Diagram of Figure 6 and Figure 8)

Below a thin surface layer exists a very low resistivity layer (0.2-1 ohm m). The layer below is rather prominently resistive (2000 ohm m) at

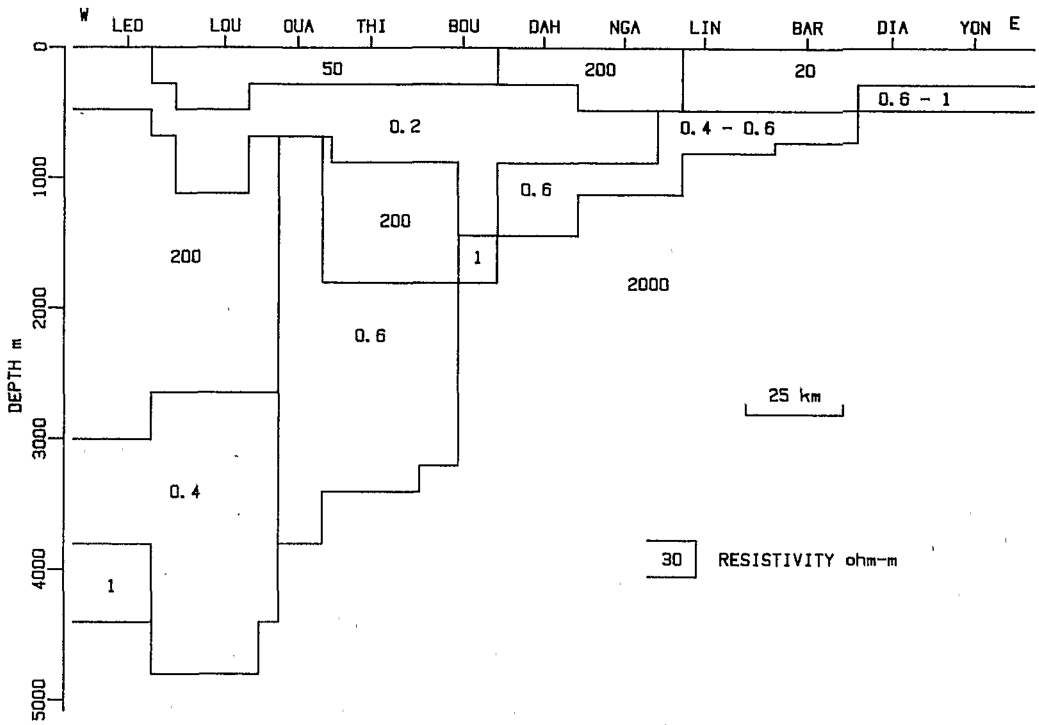

Fig. 8. Alternative geoelectrical model across the Senegal basin. The numbers give the resistivities in ohm meters.

stations BOU, DAH, NGA, LIN, BAR, DIA, and YON and probably represents the basement. For the westerly sites (deep basin), two geoelectrical models are proposed. The first model (Figure 6) shows significant lateral changes in resistivity and large uniform layers appear to be rare. Bodies with relatively high resistivity (200 ohm m) are embedded in layers of lower resistivities (0.4-0.6 ohm m) in the depth 1000-3000 m. The depth to the final conductive layer increases from east to west up to an approximate depth of 5 km at the west end of the profile. Below this conductive layer there is a resistive layer of 2000 ohm m which is believed to represent both the basement complex of Jurassic sedimentary and metamorphic rocks and the granitic crust. Below the uppermost zone the alternative model (Figure 8) shows very low resistivity layers which can be followed across the entire profile and an irregular interface between the base of the deep conductive layer and the resistive layer beneath.

On the basis of geophysical and drill hole data we propose the following explanation for the shallow low resistivity layers deduced from alternate models. The resistivity variations indicate a transition downward of fresh-water-saturated sediments near the surface to saline-water-saturated sediments above the basement; the deep conducting layer may represent a reservoir of saline fluids. The porosity of the sedimentary units and the resistivity of the contained fluids largely determine the apparent resistivities measured by the MT method.

Crust and Upper Mantle (Lower Diagram in Figure 6)

The most significant feature of the model is that a major portion of the crust, between DAH and LIN, to a depth of 4-23 km is extremely conductive with a resistivity of 2 ohm m compared to the high value of 2000 ohm m at other sites. The conductor may extend to the bottom of the crust in this region [Liger, 1980]. It is striking, however, that this main feature of the area under study have no pronounced effect on the direction of anomalous current flow at all periods shown (Figure 5). The distribution of anomalous telluric currents is influenced by deep basin fill material and does not indicate the existence of conductive structures beneath the central part of the profile. The strong lateral variation of electrical conductivity in the crust indicated by our two-dimensional model within the central part of the profile is surprising. One could speculate that a possible mechanism which explains the enhanced electrical conductivity at sites DAH, NGA, and LIN is the concentration of highly saline solutions within a large ancient fracture zone in the crust created by extensional deformation and associated with Mesozoic rifting, responsible for the formation of the Senegal basin. Such deep fractures and fissured zones in the crust have been mentioned by some workers [Jones, 1981; Adam, 1984; Adam and Pospisil,1984]. Highly conducting zones have been found throughout the world by a number of workers in different tectonic units [Tammemagi and Lilley, 1973; Greenhouse and Bailey, 1981; De Beer et al., 1982; Kurtz et al., 1982; Stanley, 1984; Gupta et al., 1985]. Other mechanisms could be proposed, such hydration process at depth [Hyndman and Hyndman, 1968], incorporation of ancient oceanic crustal material [Drury and Niblett, 1980], high temperatures [Hermance, 1983; Schwarz et al., 1984]. However, it seems impossible at this stage to arrive, on the basis of MT and DGS data only, at an unique interpretation of the crustal conductor.

In the eastern basin a layer of 200 ohm m resistivity is modeled at a depth of about 23 km; this zone may be 7 km thick and is underlain by a more resistive horizon (of the order of 2000 ohm m). A decreasing resistivity from approximately 2000-200 ohm m may be also present below the western basin at about 20 km depth. However, the insertion of this feature beneath the deep basin is poorly constrained in as much as the observed data are fitted nearly as well by a entirely resistive crust. The veracity of the 200 ohm m layer below the deep basin is therefore uncertain.

For the westerly stations no conductive layer at great depths is required to fit the observed data. Nevertheless, at depths in excess of 150 km there is a general trend toward lower resistivities, the transition from 2000 to about 2 ohm m occurs at about 175 km; a similar general decrease in resistivity also occurs for the easterly stations. Some degree of partial basalt melting has been the most frequent interpretation for conducting layers in the upper mantle at depths of about 150 km [Shankland and Waff, 1977; Lilley et al., 1981]. Another interesting feature of this geoelectric profile is the existence of a 20-km-thick layer with resistivities of about 20 ohm m at 80 km depth under the eastern basin. For the westerly sites the main traits of the deep conductivity distribution are ill-resolved because of the obscuring effect of the thick low-resistivity sediments.

Conclusions

The combined use of MT and DGS techniques shows that it has been possible to obtain the conductivity distribution of the crust and upper mantle from a traverse across the Senegal basin. This shows strong lateral variations of conductivity in the crust and the presence of regions of high conductivity at both crustal and upper mantle depths. However, for the stations inside the deep basin, fits between computed and observed data have been obtained with alternate models. This lack of resolution is attributed to ambiguity inherent in the two-dimensional models themselves. The study of the regional geomagnetic variation field indicates the presence of a concentration of telluric current which are controlled by the electrical conductivity of local geologic structures. The model interpretation of the observed features suggests that the sources of the anomalous current system are sedimentary rocks of high conductivity lying at depths of up to 5 km and a major crustal conductor situated in the central part of the profile. An interesting feature of this geoelectric profile is the confirmation of the existence of a very good crustal conductor under the margin of the deep basin, similar to the one previously reported along a traverse in the southern part of the Senegal basin [Ritz, 1984]. In general terms this is the basis for speculating a possible conductive link between the north and southern conductors along about longitude 15°30'W. Further MT and DGS studies are required to confirm this contention. Although the conductors appear to be well defined by MT studies, it should be noted that there is some uncertainty in the continuation of the current pattern southward because the differential fields near and inside the anomalous area appear to be dominated by the conductive structure of the deep basin and its characteristics cannot be determined unambiguously.

The above considerations have resulted from some simple two-dimensional models. It is understood that models for profile under study are non unique, and refinements can be made for a better overall fit to the observed data. One cannot minimize the distorsion effects of shallow three-dimensional heterogeneities on regional electromagnetic studies, and three-dimensional modeling would be necessary to evaluate quantitatively the effects of current channelling on our interpretations, since strong anomalous fields are associated with the Senegal basin.

Acknowledgments. The authors are indebted to Michel Chauvin, Michel Dukhan, and Lucien Mollard of the Geophysics Branch of the ORSTOM for technical and fieldwork assistance. We wish to express our gratitude to P. E. Wannamaker of the Earth Science Laboratory of the University of Utah Research Institute who has given his two-dimensional modeling program.

References

Adam, A., Fractures as conducting dykes and corresponding two dimensional models, Geophys. Prospect., 32, 543-553, 1984.

Adam, A., and L. Pospisil, Crustal conductivity anomalies in the Carpathian region, Acta Geod. Geophys. Mont. Hung., 19, 19-34, 1984.

Babour, K., and J. Mosnier, Direct determination of the characteristics of the current responsible for the geomagnetic anomaly of the Rhinegraben, Geophys. J. R. Astron. Soc., 60, 327-331, 1980.

Babour, K., J. Mosnier, M. Daignieres, G. Vasseur, J. L. Le Mouel, and J. C. Rossignol, A geomagnetic variation anomaly in the northern Pyrenees, Geophys. J. R. Astron. Soc., 45, 583-600, 1976.

Beamish, D., and R. J. Banks, Geomagnetic variation anomalies in northern England: Processing and presentation of data from a non-simultaneous array, Geophys. J. R. Astron. Soc., 75, 513-539, 1983.

Beblo, M., A. Bjornsson, K. Arnason, B. Stein, and P. Wolfgram, Electrical conductivity beneath Iceland: Constraints imposed by magnetotelluric results on temperature, partial melt, crust and mantle structure, J. Geophys., 53, 16-23, 1983.

Berdichevsky, M. N., and V. I. Dimitriev, Basic principles of interpretation of magnetotelluric sounding curves, in Geoelectric and Geothermal Studies, edited by A. Adam, pp. 163-221, Akademiai Kiado, Budapest, 1976.

Bureau de Recherches Petrolieres, Magnetisme aeroporte du Senegal, Report, Compagn. Gen. Geophys., Paris, 1956.

Crenn, Y., and J. Rechenmann, Mesures gravimetriques et magnetiques au Senegal et en Mauritanie occidentale, Cah. ORSTOM, Ser. Geophys., 6, 59 pp., 1965.

De Beer, J. H., J. S. V. Van Zijl, and D. I.

Gough, The southern Cape conductive belt (South Africa): Its composition, origin and tectonic significance, Tectonophysics, 83, 205-225, 1982.
De Spengler, A., J. Castelain, J. Cauvin, and M. Leroy, Le bassin secondaire-tertiaire du Senegal, in Bassins Sedimentaires du Littoral Africain, Littoral Atlantique, edited by D. Reyre, pp. 80-94, Paris, 1966.
Drury, M. J., and E. R. Niblett, Buried ocean crust and continental crust geomagnetic induction anomalies: A possible association, Can. J. Earth Sci., 17, 961-967, 1980.
Dupis, A., and A. L. Thera, Natural electromagnetism in the Rhine graben, Geophys. J. R. Astron. Soc., 68, 545-557, 1982.
Edwards, R. N., and J. P. Greenhouse, Geomagnetic variations in the eastern United States: Evidence for a highly conducting lower crust?, Science, 188, 726-728, 1975.
Fischer, G., The north Pyrenean magnetic anomaly re-examined, Ann. Geophys., 2, 181-186, 1984.
Greenhouse, J. P., and R. C. Bailey, A review of geomagnetic variation measurements in the eastern United States: Implications for continental tectonics, Can. J. Earth Sci., 18, 1268-1289, 1981.
Grillot, L. R., Calculation of the magnetotelluric tensor impedance: Analysis of band-limited MT signal pairs, Geophysics, 40, 790-797, 1975.
Gupta, J. C., R. D. Kurtz, P. A. Camfield, and E. R. Niblett, A geomagnetic induction anomaly from IMS data near Hudson Bay, and its relation to crustal electrical conductivity in central North America, Geophys. J. R. Astron. Soc., 81, 33-46, 1985.
Hermance, J. F., The asymptotic response of the three-dimensional basin offsets to magnetotelluric fields at long periods: The effects of current channeling, Geophysics, 11, 1562-1573, 1982.
Hermance, J. F., Electromagnetic induction studies, Rev. Geophys., 21, 652-665, 1983.
Hyndman, R. D., and D. W. Hyndman, Water saturation and high electrical conductivity in the lower continental crust, Earth Planet. Sci. Lett., 4, 427-432, 1968.
Jones, A. G., On a type classification of lower crustal layers under Precambrian regions, J. Geophys., 49, 226-233, 1981.
Jones, A. G., The problem of current channelling: A critical review, Geophys. Surv., 6, 79-122, 1983.
Jupp, D. L. B., and K. Vozoff, Stable iterative methods for the inversion of geophysical data, Geophys. J. R. Astron. Soc., 42, 957-976, 1975.
Kurtz, R. D., E. R. Niblett, M. Chouteau, W. J. Scott, and L. R. Newitt, An anomalous electrical resistivity zone near Ste-Mathilde, Quebec, Rep. 922, pp. 56-67, Earth Phys. Branch, Ottawa, Ont., 1982.
Liger, J. L., Structure profonde du bassin cotier senegalo-mauritanien. Interpretation de donnees gravimetriques et magnetiques, Trav Lab. Sci. Terre St.Jerome, Marseille, Ser. B, 16, 158 pp., 1980.
Liger, J. L., and J. Roussel, Etude gravimetrique du bassin cotier profond senegalais, Rev. Geol. Dynam. Geogr. Phys., 21, 419-427, 1979.
Lilley, F. E. M., D. V. Woods, and M. N. Sloane, Electrical conductivity profiles and implications for the absence or presence of partial melting beneath central and south-east Australia, Phys. Earth Planet. Inter., 25, 419-428, 1981.
Mathiez, J. P., and G. Huot, Prospection geophysique et recherches d'eaux souterraines: Exemples d'applications en Afrique orientale, Report, pp. 72-78, Com. Int. Afr. et Hydraul., Paris, 1966.
Maugis, P., L'activité de la mission de pré-reconnaissance du Bureau de Recherche de Pétrole dans les bassins sédimentaires de l'A.O.F., Rev. Inst. Fr. Pét., 9, 3-17, 1955.
Mosnier, J., and P. Yvetot, Nouveau type de variometre a aimant asservi en direction, Ann. Geophys., 28, 219-224, 1972.
Parkinson, W. D., and F. W. Jones, The geomagnetic coast effect, Rev. Geophys., 17, 1999-2015, 1979.
Pascal, M., and P. Michel, Etude geologique: Tectonique, in Notice explicative de la carte geologique au 1/200 000 Louga, pp. 5-14, Bur. Rech. Geol. Min., Dakar, 1967.
Ritz, M., Electrical resistivity structure of the Senegal basin as determined from magnetotelluric and differential geomagnetic soundings, Geophys. J. R. Astron. Soc., 79, 635-649, 1984.
Ritz, M., and R. Flicoteaux, Interpretation d'une prospection tellurique effectuee sur un profil Est-Ouest a travers le bassin meso-cenozoique senegalais, Bull. Soc. Geol. Fr., 8, 891-897, 1985.
Roussel, J., and J. L. Liger, A review of deep structure and ocean-continent transition in the Senegal basin (West Africa), Tectonophysics, 91, 183-211, 1983.
Schwarz, G., V. Haak, E. Martinez, and J. Bannister, The electrical conductivity of the Andean crust in northern Chile and southern Bolivia as inferred from magnetotelluric measurements, J. Geophys., 55, 169-178, 1984.
Shankland, T. J., and H. S. Waff, Partial melting and electrical conductivity anomalies in the upper mantle, J. Geophys. Res., 82, 5409-5417, 1977.
Sims, W., and F. Bostick, Methods of magnetotelluric analysis, Tech. Rep. 58, 86 pp., Electr. Res. Cent., Univ. of Tex., Austin, 1969.
Stanley, W. D., Tectonic study of Cascade Range and Columbia Plateau in Washington State based upon magnetotelluric soundings, J. Geophys. Res., 89, 4447-4460, 1984.
Swift, C. M. A., A magnetotelluric investigation of an electrical conductivity anomaly in the southwestern United States, Ph.D. thesis, 211 pp., Mass. Inst. of Technol., Cambridge, 1967.
Tammemagi, H. Y., and F. E. M. Lilley, A magnetotelluric traverse in southern Australia, Geophys. J. R. Astron. Soc., 31, 433-445, 1973.
Thayer, R. F., Telluric-magnetotelluric investigations of regional geothermal processes in Iceland, Ph.D. thesis, 255 pp., Brown Univ., Providence, R. I., 1975.
Vasseur, G., and P. Weidelt, Bimodal electromagnetic induction in non-uniform thin sheets with an application to the northern Pyrenean

induction anomaly, Geophys. J. R. Astron. Soc., 51, 669-690, 1977.

Vozoff, K., The magnetotelluric method in the exploration of sedimentary basins, Geophysics, 37, 98-141, 1972.

Weaver, J. T., Regional induction in Scotland: An example of three-dimensional numerical modelling using the thin sheet approximation, Phys. Earth Planet. Inter., 28, 161-180, 1982.

Wannamaker, P. E., J. A. Stodt, and L. Rijo, PW2D, Finite element program for solution of magnetotelluric responses of two-dimensional Earth resistivity structure. User documentation, Rep. DOE/SAN/12196-13, 71 pp., Dep. of Geol. and Geophys., Univ. of Utah, Salt Lake City, 1985.

Wyrobek, S. M., Reinterpretation des etudes refractions au Senegal par la S.P.S. en 58-59, Report, Soc. Petroles Senegal, Dakar, 1960.

M. Ritz and J. Vassal, ORSTOM Geophysique B.P. 1386, Dakar, Senegal.

(Received March 13, 1986;
revised May 12, 1986;
accepted May 29, 1986.)